Inflationary magnetogenesis beyond slow-roll and its induced gravitational waves

Bill Atkins[®], Debika Chowdhury[®], Alisha Marriott-Best, and Gianmassimo Tasinato^{1,3}

¹Physics Department, Swansea University, Swansea SA2 8PP, United Kingdom

²Indian Institute of Astrophysics, II Block, Koramangala, Bengaluru 560034, India

³Dipartimento di Fisica e Astronomia, Università di Bologna, INFN, Sezione di Bologna, viale B. Pichat 6/2, 40127 Bologna, Italy

(Received 8 July 2025; accepted 27 August 2025; published 19 September 2025)

The origin of magnetic fields observed on both astrophysical and cosmological scales is a compelling problem that has the potential to shed light on the early Universe. We analytically investigate inflationary magnetogenesis in scenarios where a brief departure from slow-roll inflation—akin to mechanisms proposed for primordial black hole formation—leads to enhanced magnetic field generation with a growing power spectrum. Focusing on the Ratra model, we derive an analytic bound on the growth of the magnetic field power spectrum in this context, showing that the spectral index can reach $d \ln \mathcal{P}_B/d \ln k = 4.75$ during the growth phase. This growth enables amplification from cosmic-microwave-background-safe large-scale amplitudes to values of astrophysical relevance. We further compute the stochastic gravitational wave background sourced by the resulting magnetic fields, incorporating their rich spectral features. Under suitable conditions, the induced signal exhibits a characteristic frequency dependence and amplitude within reach of future gravitational wave observatories, providing a distinctive signature of this mechanism and a specific class of templates for upcoming gravitational wave searches.

DOI: 10.1103/btjz-pqgv

I. INTRODUCTION

Understanding the origin of magnetic fields observed on large astrophysical and cosmological scales is a fascinating problem that may provide valuable insights into the early evolution of the Universe. Over the past few decades, significant efforts have been devoted to this question—see, for instance, reviews in [1-7]. An intriguing possibility is that cosmic inflation generates the seeds for the subsequent evolution of cosmic magnetic fields: References [8–16] include original and influential works on primordial magnetogenesis. However, as discussed in these works, scenarios of inflationary magnetogenesis face stringent experimental and theoretical constraints that should be carefully addressed. We adopt the scenario of Ratra [9] and consider a coupling of the inflaton field to the electromagnetic field during inflation, so as to break the conformal invariance of the Maxwell action, and to allow for magnetic field production. We link magnetogenesis to the physics of primordial black holes [see [17] for a review], by assuming that a brief phase of violation of slow-roll conditions occurs during inflation, causing the inflaton velocity to change abruptly during a short period of time. Such a non-slow-roll phase—used in the context of primordial black hole physics to enhance the spectrum of curvature fluctuations—drastically affects the time dependence of the coupling of the inflaton with Maxwell gauge fields, and influences the production of primordial magnetic fields at small scales only, with interesting phenomenological ramifications. This scenario has the potential to selectively amplify a primordial magnetic field at certain small scales. This topic has been recently investigated in [18,19], though without addressing the specific questions we consider here.

Assuming an initial nearly scale-invariant magnetic field spectrum on large scales, with an amplitude low enough to satisfy stringent constraints from cosmic microwave background (CMB) observations [20], we show that a non-slow-roll epoch can rapidly amplify the magnetic field to levels compatible with those observed in astrophysical contexts. We address two questions:

(1) Within this approach, what is the maximal possible slope of the magnetic field spectrum as it grows from large to small scales? This question is important because the magnetic field amplitude must increase by several orders of magnitude from tiny values at the largest scales—where it is constrained by CMB observations—to smaller cosmological or astrophysical scales, where observations suggest much stronger fields. An analog problem has been studied in [21] in the context of adiabatic curvature

perturbations ζ relevant for the formation of primordial black holes. There, the amplification of ζ from large to small scales was shown to be bounded by $\frac{d \ln \mathcal{P}_{\zeta}}{d \ln k} = 4$, up to subdominant logarithmic corrections [22,23]. In Sec. II, we address the analogous question for the magnetic field spectrum. We develop a fully analytical method, building on [24,26], and find that the growth rate of the magnetic field spectrum \mathcal{P}_B can exceed that of the curvature spectrum. In fact, under our assumptions, the maximal slope is $\frac{d \ln \mathcal{P}_B}{d \ln k} = 4.75$, and the resulting magnetic spectrum has a rich profile as a function of the momentum scale. We also comment how our scenario addresses strong coupling and backreaction problems of magnetogenesis.

(2) Given that our non-slow-roll mechanism leads to a rapid amplification of the magnetic field spectrum at small scales, does this process also generate vectorinduced gravitational waves (GWs) at second order in magnetic field fluctuations? The generation of GWs induced by adiabatic scalar fluctuations has a well-established history, see e.g. [27-33]: it has recently gained renewed interest as a probe of primordial black hole scenarios [see, e.g., [34] for a review]. In contrast, less attention has been given to GW production from non-adiabatic sources [see, e.g., [35–39]], although there is existing literature on GWs arising from magnetogenesis scenarios [see, e.g., [40-48]]. A common assumption in previous studies of magnetically induced GWs is that the magnetic field spectrum follows a simple powerlaw behavior. However, as outlined above, in our scenario the magnetic spectrum exhibits a much richer structure. This requires an extension of the standard formalism of magnetically induced GW to properly account for the non-trivial spectral features of our setup. In Sec. III, we present such an extension and compute the resulting GW spectrum. We find that, under suitable conditions, the amplitude of the induced GWs can be large enough to be potentially detectable by future GW observatories. The resulting GW spectrum exhibits a distinctive frequency dependence, which could serve as a characteristic signature of our scenario, helping to distinguish it from other early universe sources of GWs.

We conclude in Sec. IV, which is followed by the technical Appendix.

II. THE MAXIMAL SLOPE OF THE MAGNETIC FIELD SPECTRUM

We consider an Einstein-Maxwell Lagrangian for the electromagnetic field in an expanding universe,

$$S = \int d^4x \sqrt{-g} \left[\frac{R}{2} - \frac{I^2(\tau)}{4} F_{\mu\nu} F^{\mu\nu} \right]. \tag{2.1}$$

We set $M_{\rm Pl}=1$, and we use a mostly plus metric signature $ds^2=a^2(\tau)[-d\tau^2+d{\bf x}^2]$. We define $F_{\mu\nu}=\partial_\mu A_\nu-\partial_\nu A_\mu$ in terms of the vector potential. The overall coupling $I(\tau)$ depends on time and serves to break the conformal symmetry of Maxwell action. $I(\tau)$ usually follows a power law profile in terms of the scale factor $a(\tau)$ during inflation. Such behavior is motivated by directly coupling a function of the inflation field $\phi(\tau)$ with the Maxwell Lagrangian. In a standard setup, the scalar profiles change very slowly as functions of time, and a simple power-law behavior for $I(\tau)$ as function of time can be easily be obtained. In this work we relax this assumption, motivating and analytically investigating scenarios where $I(\tau)$ changes rapidly during inflation.

We decompose the Maxwell part of action (2.1) in terms of the spatial components A_i of the vector potential (after integrating out the auxiliary time-like component A_0)

$$S = \frac{1}{2} \int d\tau d^3x I^2(\tau) \left(A_i'^2 - \frac{1}{2} (\partial_i A_j - \partial_j A_i)^2 \right). \tag{2.2}$$

The magnetic field components scale with time as $B_i(\tau, \mathbf{x}) \propto 1/a(\tau)$ [7]. Hence, after inflation we can write the equality

$$B_i(\tau, \mathbf{x}) = a_R / a(\tau) B_i(\tau_R, \mathbf{x}), \tag{2.3}$$

where $B_i(\tau_R, \mathbf{x}) = \epsilon_{ijk} \partial_j A_k(\tau_R, \mathbf{x})$ is the value of the magnetic field right at the end of inflation.

The electromagnetic potential is decomposed in Fourier space as

$$A_i(\tau, \mathbf{x}) = \sum_{\lambda} \int \frac{d^3 \mathbf{k}}{(2\pi)^{3/2}} e^{i\mathbf{k}\cdot\mathbf{x}} \mathbf{e}_i^{(\lambda)}(\hat{k}) A_k(\tau), \qquad (2.4)$$

with $\mathbf{e}_i^{(\lambda)}$ being two polarization vectors orthogonal to the momentum \mathbf{k} . The amplitude $P_B(k)$ of the 2-point correlator for the magnetic field at the end of inflation is defined in terms of the Fourier transform of the magnetic field correlation function in Fourier space as follows:

$$\langle B_i(\tau_R, \mathbf{k}) B_i(\tau_R, \mathbf{q}) \rangle_{\mathbf{k} = \mathbf{q}}' = \pi_{ii} P_B(k),$$
 (2.5)

with

$$\pi_{ij} = \delta_{ij} - \hat{k}_i \hat{k}_j, \tag{2.6}$$

¹Stronger growth may be possible if multiple successive phases of non-slow-roll evolution are allowed [see [24]] or if the initial vacuum deviates from the Bunch–Davies form [see [25]].

and the symbol $\langle ... \rangle_{\mathbf{k}=\mathbf{q}}'$ indicates two-point correlators omitting the momentum-conserving δ -function. From now on, vectors with a hat indicate unit vectors, as $\hat{k} = \mathbf{k}/k$ with $k = \sqrt{\mathbf{k} \cdot \mathbf{k}}$. To proceed, it is convenient to rescale A_k by means of the conformal function I:

$$A_k(\tau) = I(\tau)A_k(\tau). \tag{2.7}$$

Its corresponding equation of motion reads

$$\mathcal{A}_k'' + \left(k^2 - \frac{I''}{I}\right) \mathcal{A}_k = 0. \tag{2.8}$$

Standard quantization rules can be implemented [see e.g. [10,15,18,49]] leading to the following expressions for the magnetic field energy density at the end of inflation—we call it the B spectrum:

$$\mathcal{P}_B(k) = \frac{d\rho_B}{d\ln k} = \frac{k^5}{2\pi^2 a_R^4} |\mathcal{A}_k|^2.$$
 (2.9)

Comparing with Eq. (2.5), since $P_B = k^2 |\mathcal{A}_k|^2 / I^2(\tau_R)$ at the end of inflation, we find the following relation:

$$\mathcal{P}_B(k) = \frac{k^3 I^2(\tau_R) P_B(k)}{2a_B^2 \pi^2}.$$
 (2.10)

As a warm-up example, we begin by selecting $I(\tau)=a^2(\tau)$, and impose Bunch-Davies initial conditions at small scales $|k\tau|\to\infty$. During inflation, we assume de Sitter expansion $a(\tau)=-1/(H_I\tau)$, with H_I being the constant Hubble parameter. Equation (2.8) is easily solved analytically:

$$\mathcal{A}_{k}(\tau) = \frac{3a^{2}(\tau)H_{I}^{2}}{\sqrt{2}} \frac{e^{-ik\tau}}{k^{5/2}} \left(1 + ik\tau - \frac{k^{2}\tau^{2}}{3}\right). \tag{2.11}$$

At time $\tau = \tau_R$, when inflation ends, the magnetic spectrum is

$$\mathcal{P}_B = \frac{9H_I^4}{4\pi^2} \left(1 + \frac{k^2 \tau_R^2}{3} + \frac{k^4 \tau_R^4}{9} \right). \tag{2.12}$$

Working in the limit $|k\tau_R| \ll 1$, this quantity becomes scale invariant. It is proportional to the fourth power of the inflationary Hubble parameter H_I , and can then be made very small at large scales [so as to satisfy existing stringent CMB bounds [20]].

Starting from the results of Eq. (2.12), it is interesting to enquire whether there are mechanisms that would be able to amplify the magnetic spectrum at small scales, so as to possibly relate the observed magnetic fields at astrophysical or cosmological scales with primordial magnetogenesis.

To do so, as anticipated in Sec. I, we consider scenarios in which the function $I(\tau)$ temporarily deviates from a power-law dependence on conformal time τ during inflation. Such deviations can be motivated by inflationary models that include a brief phase of non-slow-roll evolution, which are particularly relevant in setups that produce primordial black holes. An appropriate choice of the epoch where non-slow-roll occurs during inflation can enhance the magnetic field amplitude at a convenient astrophysical or cosmological scale. Hence, in what follows we will dub this possibility *non-slow-roll magnetogenesis*.

We model $I(\tau)$ as

$$I(\tau) = a^2(\tau)\sqrt{\omega(\tau)},\tag{2.13}$$

with $\omega(\tau_R)=1$ when inflation ends. If we choose $\omega(\tau)=1$ throughout all the inflationary evolution, we recover a scale invariant magnetic field spectrum as outlined above. More generally, extending the analysis of [24] from the scalar to the vector sector, we parametrize the time-dependent function $\omega(\tau)$ as

$$\omega(\tau) = \begin{cases} \omega_0 \text{ (a constant)} & \text{for } \tau < \tau_1, \\ \text{continuous but drastically changing for } \tau_1 < \tau < \tau_2, \\ 1 & \text{for } \tau_2 < \tau_R. \end{cases}$$
(2.14)

The two instants τ_1 and τ_2 during inflation are nearby, and hence we assume $(\tau_1 - \tau_2)/\tau_1 \ll 1$. Consequently, during the short time interval $\tau_1 < \tau < \tau_2$, the conformal function $I(\tau)$ can experience strong departures from a power-law profile, as dictated by Eq. (2.13). Correspondingly, a new characteristic scale

$$k_{\star} = -1/\tau_1 = a(\tau_1)H_I \tag{2.15}$$

is expected to play a relevant role in our discussion—with such a scale being associated to a comoving momentum of modes leaving the horizon at the onset of the non-slow-roll epoch during inflation. We confirm this expectation in the following discussion.

A. Analytical determination of the magnetic mode function

We now aim to solve Eq. (2.8) with a general, slow-roll-violating function $I(\tau)$ as given by Eq. (2.13). In order to

³We can consider other powers of the scale factor in Eq. (2.13), and write $I(\tau) = a^n(\tau)\sqrt{\omega(\tau)}$. The analysis that follows can be readily extended to this generalized form.

²Additionally, changes in the slope of $I(\tau)$, as the ones we consider, can help in building magnetogenesis scenarios [15] which avoid well-known strong coupling problems [11]. We elaborate further in Sec. II C.

find analytic solutions of Eq. (2.8) in the interval $\tau_1 < \tau < \tau_2$, we proceed as [24]. [See also [50,51] for different approaches to determine analytic solutions for similar setup.] We choose an ansatz $A_k(\tau)$ expanded as

$$\mathcal{A}_{k}(\tau) = \frac{3a^{2}(\tau)\sqrt{\omega(\tau)}H_{I}^{2}}{\sqrt{2}}\frac{e^{-ik\tau}}{k^{5/2}}\left[1 + ik\tau - \frac{k^{2}\tau^{2}}{3} + (ik\tau_{0})^{2}G_{(2)}(\tau) + (ik\tau_{0})^{3}G_{(3)}(\tau) + \cdots\right],\tag{2.16}$$

with τ_0 being a pivot quantity which will not appear in the final results, while $G_{(n)}(\tau)$ is a set of functions to be determined. Plugging this ansatz into Eq. (2.8), we find a system of coupled ordinary differential equations, which we aim to solve order by order in powers of k:

$$\partial_{\tau} \left(\frac{\tau_0^2 \omega}{\tau^4} G'_{(2)} \right) = \frac{\omega'}{3\tau^3}, \tag{2.17}$$

$$\partial_{\tau} \left[\frac{\omega}{\tau^4} \left(\tau_0 G'_{(3)} - G_{(2)} - \frac{\tau^2}{3\tau_0^2} \right) \right] = \frac{\omega}{\tau^4} \left(G'_{(2)} + \frac{2\tau}{3\tau_0^2} \right), \quad (2.18)$$

and for all $n \ge 4$:

$$\partial_{\tau} \left[\frac{\omega}{\tau^4} \left(\tau_0 G'_{(n)} - G_{(n-1)} \right) \right] = \frac{\omega G'_{(n-1)}}{\tau^4}.$$
 (2.19)

We follow the protocol of [24] to solve this system in the interval $\tau_1 < \tau < \tau_2$. [We refer the reader to [24] for

additional technical details.] The solution nearby τ_1 is

$$\tau_0^2 G_{(2)}(\tau) = \frac{\alpha}{3} \frac{(\tau - \tau_1)^2}{2}, \qquad (2.20)$$

$$\tau_0^n G_{(n)}(\tau) = \frac{\alpha \tau_1}{3} 2^{n-3} \frac{(\tau - \tau_1)^{n-1}}{(n-1)!}, \qquad (2.21)$$

with a constant parameter α defined as

$$\alpha = \left(\frac{d\ln\omega}{d\ln\tau}\right)_{|\tau=\tau_1}.\tag{2.22}$$

These solutions correctly describe the system in the time short interval of interest, $\tau_1 \le \tau \le \tau_2$. The dimensionless quantity α in Eq. (2.22) is a key parameter for us. If large, it can considerably amplify the magnetic spectrum from large toward small scales.

In fact, plugging the configurations (2.21) into Eq. (2.16) yields a series of the form

$$\mathcal{A}_{k}(\tau) = \frac{3a^{2}\sqrt{\omega}H_{I}^{2}e^{-ik\tau}}{\sqrt{2k^{5}}}\left[1 + ik\tau - \frac{k^{2}\tau^{2}}{3} - \frac{\alpha}{6}k^{2}(\tau - \tau_{1})^{2} - \frac{i\alpha k\tau_{1}}{12}\left(1 + 2ik(\tau - \tau_{1}) - \sum_{n=0}^{\infty}\frac{(2ik)^{n}}{n!}(\tau - \tau_{1})^{n}\right)\right]. \quad (2.23)$$

The exponential series can be resummed, yielding an exact solution:

$$\mathcal{A}_{k} = \frac{3a^{2}\sqrt{\omega}H_{I}^{2}e^{-ik\tau}}{\sqrt{2k^{5}}}\left[1 + ik\tau - \frac{k^{2}\tau^{2}}{3} - \frac{\alpha}{6}k^{2}(\tau - \tau_{1})^{2} - \frac{i\alpha k\tau_{1}}{12}(1 + 2ik(\tau - \tau_{1}) - e^{2ik(\tau - \tau_{1})})\right]. \tag{2.24}$$

This is the analytic solution of the mode function in the interval $\tau_1 < \tau < \tau_2$. Implementing Israel junction conditions, the expression (2.24) is then joined to a second period of standard power-law evolution for the conformal function $I(\tau)$ for $\tau_2 \le \tau \le \tau_R$, with τ_R being the conformal time when inflation ends. According to Eq. (2.13), in this interval we recover $I(\tau) = a^2(\tau)$ —the profile associated with a scale invariant magnetic spectrum. Recalling the definition (2.15) of k_{\star} , we introduce the convenient

dimensionless variables κ and $\Delta \tau$ as

$$\kappa = k/k_{\star} = -\tau_1 k, \tag{2.25}$$

$$\tau_2 - \tau_1 = -\tau_1 \Delta \tau. \tag{2.26}$$

The solution for the mode function in the interval $au_2 < au < au_R$ results

$$\mathcal{A}_{k} = \frac{3a^{2}(\tau)H_{I}^{2}}{2k^{5/2}} \left[C_{1}e^{-ik\tau} \left(1 + ik\tau - \frac{k^{2}\tau^{2}}{3} \right) + C_{2}e^{ik\tau} \left(1 - ik\tau - \frac{k^{2}\tau^{2}}{3} \right) \right], \tag{2.27}$$

with $C_{1,2}$ fixed by Israel conditions

$$C_{1} = 1 + 2\Delta\tau\alpha \frac{\kappa(2(\Delta\tau - 1)^{2}(\Delta\tau + 1)\kappa^{2} + 2i(\Delta\tau - 1)(3\Delta\tau + 1)\kappa - 9\Delta\tau + 2) - 6i}{8(\Delta\tau - 1)^{4}\kappa^{3}} + \alpha \frac{e^{2i\Delta\tau\kappa}(2(\Delta\tau - 1)\kappa + 3i) + 2\kappa - 3i}{8(\Delta\tau - 1)^{4}\kappa^{3}},$$
(2.28)

$$C_{2} = \frac{\alpha e^{-i(\Delta \tau - 2)\kappa} (2(\Delta \tau^{2} - 1)\kappa^{2} + i(\Delta \tau (3\Delta \tau - 5) - 4)\kappa + 6\Delta \tau + 3)\sin(\Delta \tau \kappa)}{4(\Delta \tau - 1)^{4}\kappa^{3}} + \frac{\alpha e^{-i(\Delta \tau - 2)\kappa} \Delta \tau (\kappa (4i(\Delta \tau - 1)\kappa - 3\Delta \tau + 9) + 6i)\cos(\Delta \tau \kappa)}{4(\Delta \tau - 1)^{4}\kappa^{3}}.$$

$$(2.29)$$

The magnetic field spectrum is then evaluated at the end of inflation, $\tau \to \tau_R$, using the definition in Eq. (2.9):

$$\mathcal{P}_B(k) = \frac{9H_I^4}{4\pi^2}|C_1(k) + C_2(k)|^2, \qquad (2.30)$$

neglecting terms depending on $k\tau_R$, and assuming that this quantity is small. Equations (2.27)–(2.30) are what we need for the considerations we develop next. At large scales, $\kappa \to 0$, the magnetic spectrum approaches a constant, with

an amplitude corresponding to the scale invariant case of Eq. (2.12):

$$\mathcal{P}_B(\kappa \ll 1) = \frac{9H_I^4}{4\pi^2}.$$
 (2.31)

Given the smallness of H_I in Planck units, this value easily satisfies CMB bounds. It is then straightforward to compute the amplitude of the spectrum at very small scales, finding

$$\mathcal{P}_{B}(\kappa \gg 1) = \frac{9H_{I}^{4}}{4\pi^{2}} \left[1 + \frac{\alpha\Delta\tau(1 + \Delta\tau)\{4 + \Delta\tau[\alpha - 8 + \Delta\tau(\alpha + 4)]\}\}}{4(1 - \Delta\tau)^{4}} \right]. \tag{2.32}$$

So, comparing with Eq. (2.31), we can obtain an enhancement in \mathcal{P}_B controlled by the parameter α . Such mechanism might then be able to produce small-scale magnetic fields compatible with cosmological observations, while satisfying stringent constraints at large CMB scales.

The natural question we address next is *how fast* can the magnetic spectrum increase from large [Eq. (2.31)] toward small [Eq. (2.32)] scales in this context? In what comes next, we show that there is a limitation on its growth rate.

B. The maximal growth of the spectrum: Analytical results

We proceed with the characterisation of the shape of the magnetic field spectrum in our framework which includes a brief violation of slow-roll conditions.⁴ We notice that considerable simplifications occur in the limit of infinitesimal $\Delta \tau$ [see the definition (2.26)], and very large α [see (2.22)]—yet ensuring that their product remains finite:

$$\Delta \tau \rightarrow 0$$
, $\alpha \rightarrow \infty$ but $\alpha \Delta \tau = 2\Pi_0$ with Π_0 finite. (2.33)

This limit resembles the 't Hooft limit of large N gauge theories [52] [see [26,53] for further discussions in a related inflationary context]. Then the quantities $C_{1,2}$ (2.28), (2.29) reduce to simple expressions:

$$C_1 = 1 + \left(1 - \frac{3i}{\kappa^3} - \frac{2i}{\kappa}\right)\Pi_0,$$
 (2.34)

$$C_2 = -\frac{e^{2i\kappa}(\kappa^3 + 4i\kappa^2 - 6\kappa - 3i)\Pi_0}{\kappa^3}.$$
 (2.35)

In order to study the slope of $\mathcal{P}_B(\kappa)$ in the general case, it is useful to introduce the ratio

$$\Pi(\kappa) = \frac{\mathcal{P}_B(\kappa)}{\mathcal{P}_B(\kappa \ll 1)} \tag{2.36}$$

of the spectrum evaluated at scale $\kappa = k/k_{\star}$ (with $k_{\star} = -\tau_1$), against its constant value at large scales $\kappa \ll 1$. The function $\Pi(\kappa)$ in Eq. (2.36) singles out the

⁴Recall the discussion before Eq. (2.13): we denote with "violation of slow-roll" a phase during which the conformal function $I(\tau)$ is not a simple power law, and obeys an ansatz as (2.13).

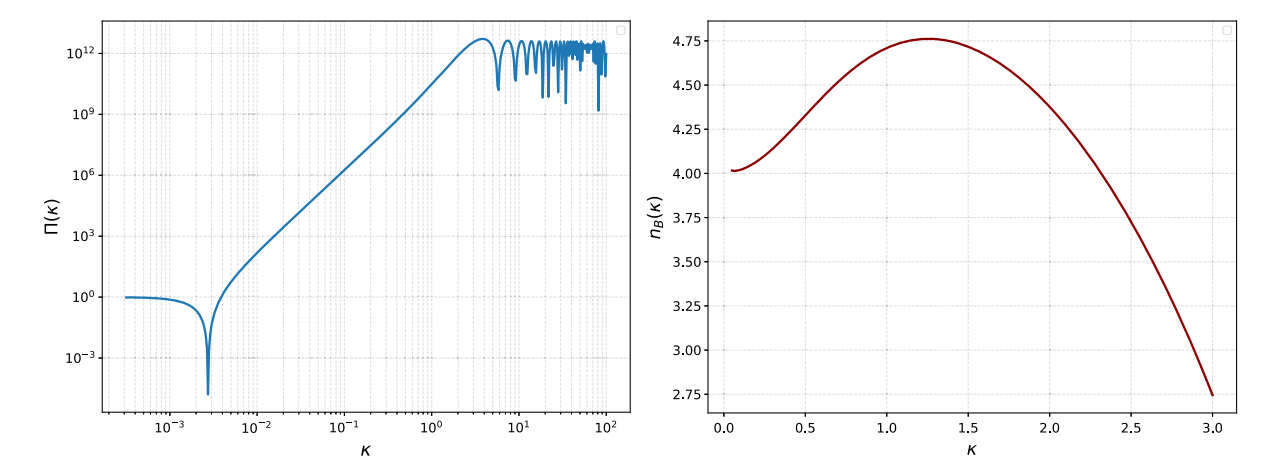


FIG. 1. Left: plot of the scale profile of the ratio (2.36) between the magnetic field spectrum against its value at large scales. We use the dimensionless variable κ , defined in Eq. (2.25), and choose $\Pi_0 = 10^6$. Right: plot of the magnetic spectral index n_B as function of the scale, Eq. (2.40), focusing on the region of growing magnetic spectrum. The spectral index has a maximum at position $\kappa_{\text{max}} \simeq 1.256$ and value $n_B(\kappa_{\text{max}}) \simeq 4.75$, after which it decreases to join the flat plateau (on average) toward small scales.

scale dependence of the spectrum. Using formula (2.32), in the limit of Eq. (2.33), this quantity results

$$\begin{split} \Pi(\kappa) = & \, 1 + \frac{2\Pi_0(\kappa^3 + [4\kappa^2 - 3)\sin(2\kappa) - (\kappa^2 - 6)\kappa\cos(2\kappa)]}{\kappa^3} \\ & + \frac{4(\kappa^2 + 1)\Pi_0^2[(\kappa^2 - 3)\sin(\kappa) + 3\kappa\cos(\kappa)]^2}{\kappa^6}. \end{split} \tag{2.37}$$

It depends on the single parameter Π_0 as defined in Eq. (2.33). In Fig. 1, left panel, we represent $\Pi(\kappa)$ as function of the dimensionless quantity κ . When expressed in terms of Π_0 , the enhancement from large toward small scales results

$$\Pi(\kappa \gg 1) = (1 + \Pi_0)^2.$$
 (2.38)

Since magnetogenesis aims to achieve an enhancement of the spectrum toward small scales, we select a large value for the dimensionless constant Π_0 (more on this in Sec. II C, where we show that Π_0 should be at least of order 10^6). At very small scales, for $\kappa\gg 1$, though, we expect that the magnetic field amplitude gets damped by dissipation or effects associated with magnetohydrodynamic (MHD) turbulence of the astrophysical plasma: see e.g. [54]. This suppression will play an important role in the analysis of induced gravitational waves in the next section.

The magnetic spectrum profile in the left panel of Fig. 1 has a dip at intermediate scales. Using the same arguments of [24,26], it is straightforward to determine its position as a function of Π_0 , in the limit of large Π_0 in which we are interested. We find

$$\kappa_{\text{dip}} = \sqrt{\frac{15}{2}} \frac{1}{\Pi_0^{1/2}},$$
(2.39)

up to corrections that are suppressed by higher powers of $1/\Pi_0$. In proceeding from small toward large κ , after the dip the magnetic field spectrum profile $\Pi(\kappa)$ grows steadily, to then join an oscillatory region with approximately constant amplitude at small scales ($\kappa \simeq 5$).

Working in the limit of large Π_0 , we can determine the spectral index associated with the magnetic field spectrum, finding

$$n_B(\kappa) = \frac{d\ln\Pi(\kappa)}{d\ln k}$$

$$= \frac{2(-3\kappa^4 + 2\kappa^2 + 9)\sin(\kappa) + 2\kappa(\kappa^4 - 5\kappa^2 - 9)\cos(\kappa)}{(\kappa^2 + 1)[(\kappa^2 - 3)\sin(\kappa) + 3\kappa\cos(\kappa)]}$$

$$+ \mathcal{O}\left(\frac{1}{\Pi_0}\right). \tag{2.40}$$

Relation (2.40) is what we need for our aim to find the maximal slope of the spectrum. The function is easy to handle, and we represent it in the right panel of Fig. 1, focusing on the region of scales where the magnetic spectrum in the figure left panel grows. We find that $n_B(\kappa)$ has a maximum at around

$$\kappa_{\text{max}} = 1.256,$$
(2.41)

where

$$n_{\text{max}}^{(B)} = n_B(\kappa_{\text{max}}) = 4.75.$$
 (2.42)

Hence, n_{max} is the maximal slope we can achieve in the specific limit (2.33) we are considering. See also the Appendix for a more systematic analysis away from the limit (2.33).

Equation (2.42) leads us to conclude that the growth of the magnetic field spectrum during a phase of

non-slow-roll—starting from a scale-invariant profile at large scales—can be steeper with respect to the case of scalar curvature fluctuations [21]. In the scalar case, the maximal slope was found to be $n_{\rm max}^{\rm (scal)}=4$, up to logarithmic corrections [22,23]. The difference among the results is due to the structure of Eq. (2.8) with $I(\tau)$ given in Eq. (2.13), which is different with respect to the scalar case. We now continue with a discussion of backreaction and strong coupling issues, to then discuss phenomenological consequences of these findings.

C. Some considerations on backreaction and strong coupling issues

In this section we estimate some features of the magnetic field spectrum produced by the non-slow-roll evolution discussed above, and we address potential issues regarding theoretical aspects of our setup. The amount of growth in the magnetic field spectrum is governed by the quantity Π_0 , depending on the slope of the conformal function $I(\tau)$ during the non-slow-roll evolution. We can estimate interesting values of Π_0 as follows. Astrophysical and cosmological observations seem to suggest that magnetic fields can be found at different astrophysical scales, with values of the order of few to tens of micro-Gauss. In this section we assume that fields of such size are produced by the primordial process we are considering, and then evolved or maintained by dynamo effects [see the review [3]].

Expressing as $\delta_B \simeq \mathcal{P}_B^{1/2}$ the size of magnetic field at the end of inflation, we have [see Eq. (2.38)]

$$\delta_B = \frac{3H_I^2}{2\pi} (1 + \Pi_0), \tag{2.43}$$

once this quantity is evaluated at small scales $k \ge k_\star$. After inflation ends, this value is rapidly diluted by cosmological expansion, with the suppression factor scaling as $(a_R/a_0)^2=10^{-29}$ assuming an instantaneous reheating process [11]. (Here a_R is the scale factor at the end of inflation, or beginning of radiation domination era, while a_0 the scale factor today.) Hence, assuming $H_I=10^{-6}$ in Planck units, and converting the results to Gauss (1 Gauss = 1.95×10^{-2} eV²), we require that the amplitude of the spectrum $\delta_B^{(0)}$ today is

$$\delta_B^{(0)} = \frac{3H_I^2}{2\pi} (1 + \Pi_0) \left(\frac{a_R}{a_0}\right)^2 = \left(\frac{\delta_B^{\text{obs}}}{10^{-5} \,\text{G}}\right) 10^{-5} \,\text{G}$$
 (2.44)

$$\simeq 10^{46} (1 + \Pi_0) (10^{-29})^2 \,\mathrm{G} = \left(\frac{\delta_B^{\text{obs}}}{10^{-5} \,\mathrm{G}}\right) 10^{-5} \,\mathrm{G}, \quad (2.45)$$

where we select a pivot value of 10 micro-Gauss for selecting a value of δ_B^{obs} compatible with astrophysical observations. Although this amplitude is larger than the required value of the seed magnetic field—typically of the order of nano-Gauss—there are various damping and diffusion mechanisms occurring in the post-inflationary universe which can dissipate the magnetic field energy over the scales of our interest [in this context, see [54,57–59]]. Solving for Π_0 , we find

$$\Pi_0 \sim 10^7 \left(\frac{\delta_B^{\text{obs}}}{10^{-5} \text{ G}} \right).$$
(2.46)

Consequently, typical values for Π_0 to obtain cosmologically significant magnetic fields at small scales span from 10^6 to few times 10^7 . Importantly, although these are the orders of magnitude of Π_0 preferred by cosmological observations, theoretical considerations prevent us from choosing Π_0 much larger than 10^6 – 10^7 . In fact, the amplitude of the magnetic field energy at small scales goes as $\rho_B \sim \mathcal{P}_B \propto H_I^2 \times (H_I \Pi_0)^2$. To avoid large backreaction on the inflationary dynamics, whose typical energy scale is of the order $\rho_{\rm inf} \sim H_I^2$, the factor $H_I \Pi_0$ can be at most of order one. Hence choosing $H_I \sim 10^{-6}$ in Planck units, we cannot select too large values of Π_0 .

The characteristic comoving momentum $k_{\star} = -1/\tau_1$, around which the rapid growth of the spectrum occurs—see Fig. 1—is determined by the time τ_1 at which a brief non-slow-roll phase takes place during inflation. Depending on the location of k_{\star} , magnetic fields can be amplified on a range of scales, from large distances corresponding to galaxy clusters (10²⁴ cm) to relatively small stellar ones (10¹⁰ cm).

Our configuration, in which the gauge kinetic function $I(\tau)$ undergoes a rapid change during a short interval, resonates with scenarios such as those proposed in [15], where a sawtooth profile for $I(\tau)$ is shown to mitigate the strong coupling problem in primordial magnetogenesis [11] [see also [60] for alternative approaches to this issue]. In essence, the problem is the following: if one chooses a function $I(\tau)$ that increases during inflation—as in the scale-invariant case $I(\tau) = a^2(\tau)$ —and imposes $I(\tau_R) = 1$ at the end of inflation, then inevitably $I(\tau)$ is extremely small at early times. Since $I(\tau)$ is inversely proportional to the electromagnetic coupling, this leads to an unphysically large coupling at early times, rendering the electromagnetic theory unreliable.

A proposed resolution [15] involves constructing scenarios in which $I(\tau)$ changes its slope during inflation, keeping its amplitude sufficiently large to avoid strong coupling throughout. In our model, a similar mechanism is potentially operative: by choosing a sufficiently large value of ω_0 in Eq. (2.14), we ensure that $I(\tau)$ remains large enough at the onset of inflation. Furthermore, if the non-slow-roll phase begins sufficiently late—that is, if τ_1 is

⁵Preliminary investigations of the analogous questions in the spin-2 (tensor) case have been presented in [55,56].

chosen appropriately—then $I(\tau)$ remains at safe values thereafter, ensuring theoretical control of the setup.⁶ It would be interesting to further develop these preliminary ideas within a fully developed framework.

III. GRAVITATIONAL WAVES INDUCED BY MAGNETIC FIELD AMPLIFICATION

In the previous sections, we learned that a period of nonslow-roll evolution can amplify the magnetic field spectrum toward small scales, at around a comoving scale k_{\star} = $-1/\tau_1$ corresponding to the brief inflationary epoch during which slow-roll is violated. In this section, we analyze the properties of GWs sourced by such an amplified magnetic field. We show that the frequency dependence of the induced stochastic GW background (SGWB) can constitute a distinct experimental smoking gun for this scenario. Interestingly, even if the magnetic field is rapidly damped by turbulence or diffusion after its production, the gravitational waves it induces can still serve as evidence of its existence in the first place. Our findings provide specific templates for SGWB profiles [see, e.g., [61-63]], highlighting inflationary magnetogenesis as a compelling target for gravitational wave searches.

To compute the induced GW spectrum, we follow the methods developed in [29,33] in the context of SGWBs in scalar-induced scenarios where amplified curvature fluctuations source the GW after inflation ends. This subject has a long history—see e.g. [27–33] and [34] for a comprehensive review. We apply the idea to the non-adiabatic case of magnetic field sources, a topic studied in several works [40–48], although usually focusing on simple power law profiles for the magnetic field correlator \mathcal{P}_B in Eq. (2.9). Here we consider much richer scale-dependent profiles for \mathcal{P}_B , as motivated by the considerations of Sec. II on non-slow-roll evolution during inflation; hence we need to further develop the corresponding formalism for GW production.

A. The calculation of the gravitational wave spectrum

After inflation ends, the GW equation of motion reads

$$h_{ij}^{\prime\prime}(\tau, \mathbf{x}) + 2\mathcal{H}(\tau)h_{ij}^{\prime}(\tau, \mathbf{x}) - \nabla^2 h_{ij}(\tau, \mathbf{x}) = \Pi_{ij}^{(T)}(\tau, \mathbf{x}),$$

$$(3.1)$$

with $\Pi_{ij}^{(T)}$ being the transverse-traceless component of the magnetic field stress tensor sourcing the GW. In order to

express this quantity and proceed with our discussion, it is convenient to work in Fourier space. The spin-2 GW fluctuations are decomposed as

$$h_{ij}(\tau, \mathbf{x}) = \sum_{\lambda} \int \frac{d^3 \mathbf{k}}{(2\pi)^{3/2}} e^{i\mathbf{k}\cdot\mathbf{x}} \mathbf{e}_{ij}^{(\lambda)}(\mathbf{k}) h_{\mathbf{k}}^{(\lambda)}, \quad (3.2)$$

with $\mathbf{e}_{ij}^{(\lambda)}(\mathbf{k})$ being the spin-2 polarization tensors. The evolution equation for the modes $h_{\mathbf{k}}^{(\lambda)}$ results

$$h_{\mathbf{k}}^{(\lambda)''} + 2\mathcal{H}h_{\mathbf{k}}^{(\lambda)'} + k^2 h_{\mathbf{k}}^{(\lambda)} = S^{(\lambda)}(\tau, \mathbf{k}). \tag{3.3}$$

The source in the right-hand side of this equation reads

$$S^{(\lambda)}(\tau, \mathbf{k}) = \mathbf{e}^{(\lambda)ij}(\hat{k})\Pi_{ij}^{(T)}(\tau, \mathbf{k}) = \frac{2\mathbf{e}^{(\lambda)ij}(\hat{k})\Lambda_{ij}^{mn}\tau_{mn}^{(B)}(\mathbf{k})}{a^{2}(\tau)},$$
(3.4)

where the magnetic field stress tensor is [see e.g. [42]]

$$\tau_{ij}^{(B)}(\mathbf{k}) = \frac{1}{4\pi} \int \frac{d^3 p}{(2\pi)^3} \left[B_i(\mathbf{p}) B_j(\mathbf{k} - \mathbf{p}) - \frac{\delta_{ij}}{2} B_m(\mathbf{p}) B_m(\mathbf{k} - \mathbf{p}) \right]. \tag{3.5}$$

The projection tensor Λ_{ij}^{mn} selects its transverse-traceless part, and is given by

$$\Lambda_{ij}^{\ell m} = \frac{1}{2} (\pi_i^{\ell} \pi_j^{m} + \pi_j^{\ell} \pi_i^{m} - \pi_{ij} \pi^{\ell m}), \text{ with } \pi_{ij} = \delta_{ij} - \hat{k}_i \hat{k}_j.$$
(3.6)

Notice that $\Lambda_{ii}^{\ell n} = \Lambda_{ij}^{\ell \ell} = 0$. Hence, we can neglect the contribution proportional to δ_{ij} in (3.5). The quantities entering Eq. (3.5) are evaluated at the end of inflation. Their value then redshifts with the universe expansion after inflation ends, as indicated by the scale factor dependence of the source (3.4).

Equation (3.3) can be formally solved as

$$h_{\mathbf{k}}^{(\lambda)}(\tau) = \frac{1}{a(\tau)} \int d\tau' g_k(\tau, \tau') [a(\tau') S_{\mathbf{k}}^{(\lambda)}(\tau')], \quad (3.7)$$

where the g_k is the Green function evaluated at the epoch of interest. During radiation domination—the era on which we focus our attention from now on—it reads

$$g_k(\tau, \tau') = \frac{1}{k} [\sin(k\tau)\cos(k\tau') - \sin(k\tau')\cos(k\tau)]. \quad (3.8)$$

⁶Alternatively, one might consider multiple short non-slow-roll epochs [24], stitched together by segments in which $I(\tau)$ follows different power-law behaviors. This would allow one more flexibility in choosing τ_1 .

The result (3.7) allows us to formally express the tensor power spectrum as

$$\mathcal{P}_{h}(\tau, k) \equiv \frac{1}{2} \frac{k^{3}}{2\pi^{2}} \sum_{\lambda} \langle h_{\mathbf{k}}^{(\lambda)}(\tau) h_{\mathbf{q}}^{(\lambda)}(\tau) \rangle_{\mathbf{k}=\mathbf{q}}^{\prime}$$
 (3.9)

$$= \frac{k^3}{4\pi^2 a^2(\tau)} \int d\tau_1 d\tau_2 g_k(\tau, \tau_1) g_q(\tau, \tau_2) a(\tau_1) a(\tau_2)$$

$$\times \left(\sum_{\mathbf{k}} \langle S_{\mathbf{k}}^{(\lambda)}(\tau_1) S_{\mathbf{q}}^{(\lambda)}(\tau_2) \rangle_{\mathbf{k}=\mathbf{q}}' \right), \tag{3.10}$$

where as before the symbol $\langle ... \rangle'_{k=q}$ indicates two-point correlators omitting the momentum-conserving δ -function. The GW spectrum above is the necessary ingredient to compute the GW density parameter, Ω_{GW} , which is the basic quantity to be compared with experiments. Following the notation of [33], we have

$$\Omega_{\rm GW} \equiv \frac{k^2}{12a^2H^2} \bar{\mathcal{P}}_h,\tag{3.11}$$

where a bar indicates the average over rapid oscillations. To proceed, we need to estimate \bar{P}_h . We compute the quantity within parenthesis in Eq. (3.10):

$$\sum_{\lambda} \langle S_{\mathbf{k}}^{(\lambda)}(\tau_{1}) S_{\mathbf{q}}^{(\lambda)*}(\tau_{2}) \rangle_{\mathbf{q}=\mathbf{k}}' \\
= \frac{4\Lambda_{ij}^{\ell n}}{a^{2}(\tau_{1})a^{2}(\tau_{2})} \langle \hat{\tau}^{(B)ij}(\mathbf{k}) \hat{\tau}_{\ell n}^{(B)*}(\mathbf{p}) \rangle_{\mathbf{p}=\mathbf{k}}' \\
= \frac{4}{(4\pi)^{2}a^{2}(\tau_{1})a^{2}(\tau_{2})} \\
\times \int \frac{d^{3}p_{1}}{(2\pi)^{3}} \Lambda_{ij}^{\ell n}(\hat{k}) (\pi_{\ell}^{i}(\hat{p}_{1})\pi_{n}^{j}(\hat{n}) + \pi_{n}^{i}(\hat{p}_{1})\pi_{\ell}^{j}(\hat{n}))$$
(3.12)

where we introduce the unit tensor $\hat{n} = (\mathbf{k} - \mathbf{p}_1)/|\mathbf{k} - \mathbf{p}_1|$, and the amplitude of the magnetic field 2-point correlators is introduced in Eq. (2.5). We do not consider non-Gaussian contributions, such as those arising from connected four-point functions of the magnetic field, since the underlying Maxwell action is quadratic in the vector fields and therefore does not generate intrinsic non-Gaussianity. Following [29,33], we introduce convenient variables

 $\times P_B(p_1)P_B(|\mathbf{k}-\mathbf{p}_1|),$

$$u \equiv \frac{|\mathbf{k} - \mathbf{p}_1|}{k}, \quad v \equiv \frac{p_1}{k}, \quad \mu \equiv \frac{\mathbf{k} \cdot \mathbf{p}_1}{k p_1} = \frac{1 - u^2 - v^2}{2v}.$$
 (3.14)

The tensors within the integral of Eq. (3.13) can be contracted straightforwardly [44], leading to a function of (u, v) which we call C_0 :

$$C_0(u,v) = \Lambda_{ii}^{\ell n}(\hat{k})(\pi_{\ell}^i(\hat{p}_1)\pi_n^j(\hat{n}) + \pi_n^i(\hat{p}_1)\pi_{\ell}^j(\hat{n}))$$
(3.15)

$$= (1 + \mu^2) \left(1 + \frac{(1 - \mu v)^2}{u^2} \right). \tag{3.16}$$

By expressing $d^3 p_1 = 2\pi p_1^2 dp_1 d\mu$, we can rewrite (3.13) as

$$\begin{split} & \sum_{\lambda} \langle S_{\mathbf{k}}^{(\lambda)}(\tau_{1}) S_{\mathbf{q}}^{(\lambda)}(\tau_{2}) \rangle' \\ & = \frac{k^{3}}{4\pi^{2} a^{2}(\tau_{1}) a^{2}(\tau_{2})} \int_{0}^{\infty} v^{2} dv \int_{-1}^{1} d\mu P_{B}(ku) P_{B}(kv) \mathcal{C}_{0}(u, v) \\ & = \frac{\pi^{2} k^{-3}}{a^{2}(\tau_{1}) a^{2}(\tau_{2})} \int_{0}^{\infty} \frac{dv}{u^{3} v} \int_{-1}^{1} d\mu \mathcal{P}_{B}(ku) \mathcal{P}_{B}(kv) \mathcal{C}_{0}(u, v), \end{split}$$

$$(3.17)$$

where we used Eq. (2.10) to pass from P_B to \mathcal{P}_B between the first and the second line. Equation (3.17) can be plugged into the definition of \mathcal{P}_h in (3.10). The tensor spectrum is then nicely factorized into two integral contributions. They are

$$\mathcal{P}_h = \frac{1}{4a^2(\tau)} \mathcal{I}_{\tau}^2 \mathcal{I}_{uv}, \tag{3.18}$$

with

$$\mathcal{I}_{\tau}^{2} = \left(\int_{\tau_{R}}^{\tau} d\tau_{1} \frac{g_{k}(\tau, \tau_{1})}{a(\tau_{1})}\right)^{2}, \tag{3.19}$$

$$\mathcal{I}_{uv} = \int_0^\infty \frac{dv}{u^3 v} \int_{-1}^1 d\mu \mathcal{P}_B(ku) \mathcal{P}_B(kv) \mathcal{C}_0(u, v). \quad (3.20)$$

We start handling the time integral in Eq. (3.19). Working in radiation domination, we use the identities $a(\tau)/a(\tau_1) = \tau/\tau_1$ and $a(\tau)H(\tau) = 1/\tau$. A simple calculation, averaging over rapid oscillations, gives at large τ :

$$\bar{\mathcal{I}}_{\tau}^{2} = \frac{1}{2k^{2}a^{4}H^{2}} \left[\text{Ci}(-k\tau_{R})^{2} + \left(\frac{\pi}{2} - \text{Si}(-k\tau_{R})\right)^{2} \right], \quad (3.21)$$

where Ci(x), Si(x) are the cosine and sine integral functions, and with the bar we average over rapid oscillations. The integral in Eq. (3.20) is conveniently expressed in terms of variables t, s:

$$u = \frac{t+s+1}{2}, \qquad v = \frac{t-s+1}{2}.$$
 (3.22)

Taking into account the corresponding Jacobian, we can write it as

$$\mathcal{I}_{uv} = \int_0^\infty dt \int_{-1}^1 ds (1 - s + t)^{-2} (1 + s + t)^{-2} \times \mathcal{P}_B(ku) \mathcal{P}_B(kv) \mathcal{C}_0(t, s),$$
 (3.23)

with

$$C_0(t,s) = \left(\frac{(s^2 + t(t+2) - 1)^2}{4(-s+t+1)^2} + 1\right) \times \left(\frac{(s^2 + t(t+2) + 3)^2}{4(s+t+1)^2} + 1\right).$$
(3.24)

We can pass from the tensor spectrum to the GW density parameter Ω_{GW} , given by Eq. (3.11). Using our formulas, we obtain:

$$\Omega_{\rm GW} = \frac{k^2}{96a^4H^2} \bar{\mathcal{I}}_{\tau}^2 \mathcal{I}_{uv}.$$
 (3.25)

We substitute into Eq. (3.25) the results derived above. We use the same expression of [41]

$$a(\tau) = H_0 \sqrt{\Omega_{\rm rd}} \tau, \tag{3.26}$$

for the scale factor during radiation domination, with H_0 and $\Omega_{\rm rd}$ being, respectively, the Hubble parameter and the fraction of total energy density in radiation. We denote with $\hat{\Omega}_B = \rho_B/\rho_{\rm cr} = \mathcal{P}_B^{\rm CMB}/(3H_0^2)$ a quantity parametrizing the fractional energy density of the magnetic field at very large CMB scales, and we use the expression (2.31) for $\mathcal{P}_B^{\rm CMB}$.

Finally, we multiply the resulting Ω_{GW} by the factor Ω_{rd} , in order to take into account the redshift of the GW observable from early to late times [see e.g. [34]]. Expressing the formulas in terms of the dimensionless κ [see Eq. (2.25)], we get

$$\Omega_{\rm GW}(\kappa) = \left[\frac{3\hat{\Omega}_B^2}{64\Omega_{\rm rd}} \right] \times \left\{ \left(\text{Ci}^2(\kappa x_{\star}) + \left(\frac{\pi}{2} - \text{Si}(\kappa x_{\star}) \right)^2 \right) \tilde{\mathcal{I}}_{uv}(\kappa) \right\},$$
(3.27)

with

$$\tilde{\mathcal{I}}_{uv}(\kappa) = \int_0^\infty dt \int_{-1}^1 ds (1 - s + t)^{-2} (1 + s + t)^{-2} \times \Pi(\kappa u) \Pi(\kappa v) \mathcal{C}_0(t, s).$$
(3.28)

The function $\Pi(x)$ is defined in Eq. (2.37), while we introduce the (small) number $x_{\star} = \tau_R/\tau_1$ which controls the ratio between the time when inflation ends versus the time $|\tau_1|$ when the slow-roll conditions are violated during inflation. This quantity only enters in the arguments of the Ci, Si functions. For clarity, we choose $x_{\star} = 10^{-4}$, but the results are in any case mildly dependent on this quantity since, when small, it enters only logarithmically in Eq. (3.27) (through Ci(x) ~ ln(x) for very small x).

The overall constant quantity [...] within square brackets in Eq. (3.27) depends on the scale of inflation, as well as on postinflationary evolution. It is the same overall constant scale found in previous works [starting with [41]] which quantifies the impact of the amplitude of large scale magnetic fields into GW observables. The overall amplitude is not our primary focus here; instead, we are interested in the scale dependence of the gravitational wave background. For definiteness, we fix the overall prefactor in Eq. (3.27) to a small value, [...] $\simeq 2 \times 10^{-48}$, to better highlight the subsequent growth of the spectrum toward smaller scales. Such reduced values can be due by post-inflationary processes related with field evolution and dissipation in the astrophysical plasma—a subject that we do not touch here, though.

The quantity within curly parenthesis $\{...\}$ in Eq. (3.27) is dimensionless, and depends on the function $\Pi(\kappa)$ which—as we learned in the previous section—controls the growth of the magnetic field spectrum. The combination within $\{...\}$ can be evaluated numerically: we find that it has a profile with a plateau, and a maximal value scaling with Π_0 as

$$\{\dots\}_{\text{max}} \simeq 10^5 \Pi_0^4.$$
 (3.29)

Using this information, we plot in Fig. 2 the resulting expression for the fractional energy density $\Omega_{\rm GW}$ in gravitational waves as a function of frequency, employing the relation $k/{\rm Mpc^{-1}} \simeq 6.5 \times 10^{14}~f/{\rm Hz}$. We choose $\Pi_0 = 7 \times 10^7$, a large value consistent with our considerations in Sec. II B. To account for the damping of the magnetic field at small scales, as anticipated in Sec. II, we truncate the magnetic power spectrum at large κ , where its amplitude is known to be suppressed by dissipation and turbulent effects [see, e.g., the review [6]]. Specifically, as a concrete example, we use the expression for $\Pi(\kappa)$ from Eq. (2.37), but set $\Pi(\kappa) = 0$ for $\kappa > 50$.

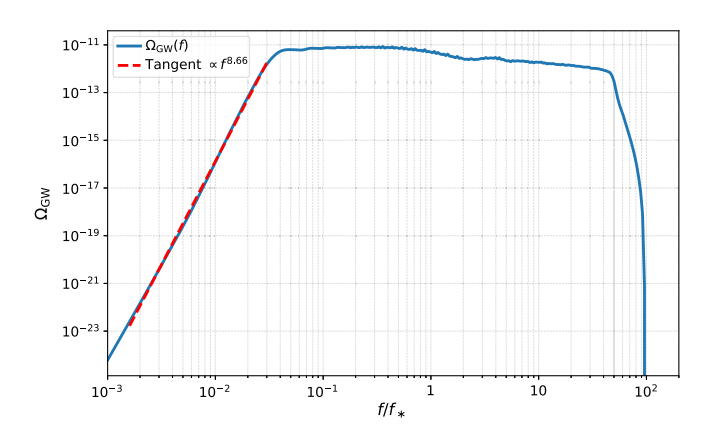


FIG. 2. Plot of $\Omega_{\rm GW}(f)$ in our setup. We follow Eq. (3.27) and choose the parameters as explained in the main text.

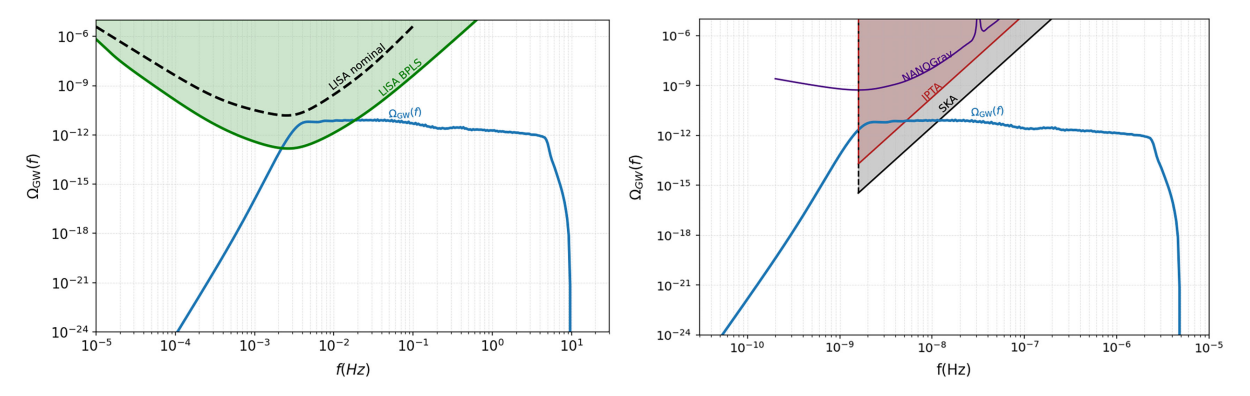


FIG. 3. Left: same frequency profile of $\Omega_{\rm GW}(f)$ as in Fig. 2 is shown for $f_{\star}=0.1$, compared against the nominal LISA sensitivity curve and its broken power-law version [66,67]. Right: same frequency profile of $\Omega_{\rm GW}(f)$ as in Fig. 2 is shown for $f_{\star}=5\times 10^{-8}$, compared against the SKA, IPTA, NANOGrav sensitivity curves.

The spectral shape of the SGWB, $\Omega_{\rm GW}(f)$, pleasantly reflects the underlying profile of the magnetic field power spectrum $\Pi(\kappa)$ that sources it:

- (i) At relatively low frequencies, $\Omega_{\rm GW}(f)$ exhibits a steep rise, scaling approximately as $(f/f_{\star})^{8.7}$. This behavior arises from the convolution integrals of Eq. (3.28), involving the square of the magnetic field spectrum. Since $\Pi(\kappa)$ during its growth scales with a spectral slope of order 4 (or slightly larger), taking its square within the integrals leads to the aforementioned scaling in the gravitational wave signal.
- (ii) This rapid growth is abruptly halted at around $f/f_{\star} \sim 1/50$, giving way to a flat plateau in the SGWB spectrum of Fig. 2. The amplitude of this plateau scales as Π_0^4 . It corresponds to the convolution of the nearly flat region of the magnetic field spectrum at small scales, which follows the initial growth phase—modulo oscillations in the magnetic field spectrum, which are smoothed out in the convolution integrals.
- (iii) At higher frequencies, specifically for $f/f_{\star} \gtrsim 10^2$, the SGWB spectrum undergoes a sharp decline. This reflects the assumed rapid suppression of $\Pi(\kappa)$ at large $\kappa \geq 50$, due to dissipation and turbulence effects in the plasma [see discussion following Eq. (3.29)]. We emphasize though that this decline in $\Omega_{\rm GW}(f)$ is model dependent, since it relies on our assumptions about the suppression of the magnetic field spectrum toward small scales.

B. Consequences for gravitational wave experiments

The selected value of the parameter $\Pi_0 = 7 \times 10^7$ leads to a gravitational wave signal with peak amplitude $\Omega_{GW} \simeq 10^{-11}$, given our hypothesis on the overall constant factor in Eq. (3.27).

This GW signal could fall within the sensitivity range of future GW experiments provided that the frequency f_{\star} determining the position of the plateau in $\Omega_{\rm GW}$ lies within

their observational bands. As specific simple examples, we show in the left panel of Fig, 3 that such a GW spectrum can be in principle detected with LISA [64], by choosing the pivot frequency $f_{\star}=0.1$ Hz. Such a pivot frequency corresponds to a magnetic field enhanced at very small scales of 3×10^{11} cm, i.e. stellar-size scales. In the right panel of Fig. 3 we instead consider a pivot frequency $f_{\star}=5\times10^{-8}$ Hz, corresponding to signals at nano-Hertz scales detectable with pulsar timing array experiments—we take the corresponding sensitivity curves from [65]. The magnetic field gets then enhanced a scales of 6×10^{17} cm, i.e. interstellar size.

The resulting SGWB spectrum has a distinctive shape: its rapid growth toward its plateau and squared shape are quite atypical compared to standard templates commonly considered in scalar-induced SGWB scenarios [63] based on adiabatic perturbations. The characteristic knee in the profile of Fig. 3 can be detected implementing techniques as [69,70]. Despite the differences between adiabatic and nonadiabatic sources, the properties of the magnetic field source can, in principle, be reconstructed using recently developed tools such as those presented in [71,72]. A more detailed analysis of the detectability and characterization of the magnetically induced SGWB will be pursued in future work: nevertheless our investigation already shows how the rich scale dependence of the magnetic field spectrum in our setup leads to a distinctive GW signal.

IV. CONCLUSIONS

We analytically investigated inflationary magnetogenesis in the Ratra model, focusing on scenarios where a brief violation of slow-roll conditions enhances the coupling between the inflaton and gauge fields. This mechanism

⁷In particular, the logarithmic slope $\ln(f/f_{\star}) \sim 8$ characterizes the spectral shape in the intermediate regime approaching the plateau, whereas in the deep infrared, the spectrum exhibits a gentler power-law behavior [68].

allows for a rapid growth of the magnetic field spectrum, with an analytically derived maximal slope of $d \ln \mathcal{P}_B / d \ln k = 4.75$, sufficient to bridge the gap between CMB-constrained large-scale amplitudes and observed astrophysical field strengths. We also commented on strong coupling and backreaction problems in this setup.

We then studied the stochastic gravitational wave background induced by the amplified magnetic fields, extending standard formalisms to account for the nontrivial spectral features of our scenario. Under suitable conditions, the resulting gravitational wave signal exhibits a characteristic frequency profile and potentially detectable amplitude, providing a unique observational handle on inflationary magnetogenesis with transient non-slow-roll dynamics.

At the technical level, the main highlights of our results are as follows:

- (i) We introduced a systematic method for analytically studying the spectral profile of perturbations for fields with spin greater than zero, and applied it to the vector case. This method yields compact analytical expressions and allows us to extract key features of the spectrum, such as the location of the dip and the rate of its growth.
- (ii) We derived general expressions for the gravitational wave spectrum induced at second order by magnetic fields, applicable to scenarios with s magnetic field profiles like ours. Remarkably, the resulting formulas exhibit a simpler, factorizable structure than their scalar, adiabatic counterparts—a feature that may prove useful for future analyses of related scenarios.

Our findings suggest a possible connection between primordial magnetogenesis, primordial black hole phenomenology, and gravitational wave physics, motivating further exploration of inflationary scenarios beyond slow-roll and their couplings with vector fields.

ACKNOWLEDGMENTS

It is a pleasure to thank Pritha Bari, Anish Ghoshal, Lorenzo Giombi, Germano Nardini, Marco Peloso and H. V. Ragavendra for useful discussions. We are partially funded by STFC Grants No. ST/T000813/1 and No. ST/X000648/1. D. C. would like to thank the Indian Institute of Astrophysics and the Department of Science and Technology, Government of India, for support through the INSPIRE Faculty Fellowship Grant No. DST/INSPIRE/04/2023/000110.

DATA AVAILABILITY

No data were created or analyzed in this study.

APPENDIX: FINITE DURATION OF THE NON-SLOW-ROLL EPOCH

In this appendix we reconsider the problem of determining the maximal slope of the magnetic field spectrum in its

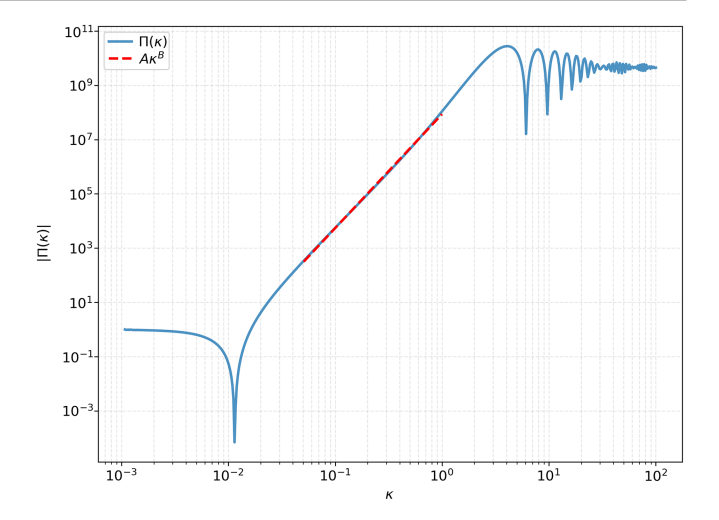


FIG. 4. Example of the fitted spectrum, $\Pi(\kappa)$, taking $\alpha = 10^7$, $\Delta \tau = 0.1$. The power-law fit finds $A = 8.9 \times 10^7$ B = 4.197.

growing region, without taking the limit of Eq. (2.33). In other words, we vary both parameters α and $\Delta \tau$, performing a grid-search, computing the maximal slope of $\Pi(\kappa)$ for choices of α and $\Delta \tau$ restricting such that $10^4 \le \alpha \Delta \tau \le 10^8$. In the growing region we assume the spectrum to follow a power-law profile $A\kappa^B$. Figure 4 explicitly shows the region in which the power law is fitted, away from deviations from linearity toward the extreme ends of the transitionary phase.

Figure 5 demonstrates the variation of the power-law exponent with the choices of α and $\Delta \tau$. In the limit that $\Delta \tau \to 0$ and $\alpha \to \infty$ we find that $B \to 4.4$. For this subspace, we find the global maximum slope be B = 4.398 for $\Delta \tau = 7 \times 10^{-4}$, $\alpha = 1.33 \times 10^{7}$. Observably, the resulting slope is smaller than the value B = 4.75 quoted in the main

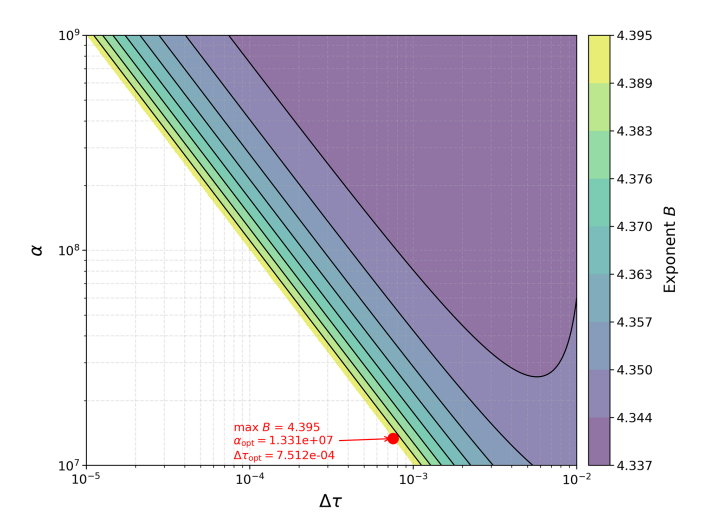


FIG. 5. Maximum slope value as function of α and $\Delta \tau$ restricted such that $10^4 \le \alpha \Delta \tau \le 10^8$. Global maximum slope found to be B = 4.395 at $\Delta \tau = 7.5 \times 10^{-4}$, $\alpha = 1.33 \times 10^7$.

text, obtained in the limit (2.33). We interpret the discrepancy as due to the fact that in this appendix we assume a power-law behavior with constant B for the entire growing part of the spectrum; however it is anticipated that the

corresponding spectral index has a nontrivial dependence on the scale—as seen for example in Fig. 1, right panel. It is intended that a more systematic analysis of this topic will be left to future work.

- [1] P. P. Kronberg, Extragalactic magnetic fields, Rep. Prog. Phys. **57**, 325 (1994).
- [2] D. Grasso and H. R. Rubinstein, Magnetic fields in the early universe, Phys. Rep. **348**, 163 (2001).
- [3] L. M. Widrow, Origin of galactic and extragalactic magnetic fields, Rev. Mod. Phys. **74**, 775 (2002).
- [4] A. Kandus, K. E. Kunze, and C. G. Tsagas, Primordial magnetogenesis, Phys. Rep. **505**, 1 (2011).
- [5] L. M. Widrow, D. Ryu, D. R. G. Schleicher, K. Subramanian, C. G. Tsagas, and R. A. Treumann, The first magnetic fields, Space Sci. Rev. 166, 37 (2012).
- [6] R. Durrer and A. Neronov, Cosmological magnetic fields: Their generation, evolution and observation, Astron. Astrophys. Rev. 21, 62 (2013).
- [7] K. Subramanian, The origin, evolution and signatures of primordial magnetic fields, Rep. Prog. Phys. 79, 076901 (2016).
- [8] M. S. Turner and L. M. Widrow, Inflation produced, large scale magnetic fields, Phys. Rev. D 37, 2743 (1988).
- [9] B. Ratra, Cosmological 'seed' magnetic field from inflation, Astrophys. J. Lett. **391**, L1 (1992).
- [10] J. Martin and J. Yokoyama, Generation of large-scale magnetic fields in single-field inflation, J. Cosmol. Astropart. Phys. 01 (2008) 025.
- [11] V. Demozzi, V. Mukhanov, and H. Rubinstein, Magnetic fields from inflation?, J. Cosmol. Astropart. Phys. 08 (2009) 025.
- [12] S. Kanno, J. Soda, and M. Watanabe, Cosmological magnetic fields from inflation and backreaction, J. Cosmol. Astropart. Phys. 12 (2009) 009.
- [13] K. Bamba and M. Sasaki, Large-scale magnetic fields in the inflationary universe, J. Cosmol. Astropart. Phys. 02 (2007) 030.
- [14] N. Barnaby, R. Namba, and M. Peloso, Observable non-Gaussianity from gauge field production in slow roll inflation, and a challenging connection with magnetogenesis, Phys. Rev. D 85, 123523 (2012).
- [15] R. J. Z. Ferreira, R. K. Jain, and M. S. Sloth, Inflationary magnetogenesis without the strong coupling problem, J. Cosmol. Astropart. Phys. 10 (2013) 004.
- [16] R. J. Z. Ferreira, R. K. Jain, and M. S. Sloth, Inflationary magnetogenesis without the strong coupling problem II: Constraints from CMB anisotropies and B-modes, J. Cosmol. Astropart. Phys. 06 (2014) 053.
- [17] O. Özsoy and G. Tasinato, Inflation and primordial black holes, Universe 9, 203 (2023).
- [18] S. Tripathy, D. Chowdhury, R. K. Jain, and L. Sriramkumar, Challenges in the choice of the nonconformal coupling function in inflationary magnetogenesis, Phys. Rev. D 105, 063519 (2022).

- [19] S. Tripathy, D. Chowdhury, H. V. Ragavendra, R. K. Jain, and L. Sriramkumar, Circumventing the challenges in the choice of the nonconformal coupling function in inflationary magnetogenesis, Phys. Rev. D 107, 043501 (2023).
- [20] P. A. R. Ade *et al.* (Planck Collaboration), Planck 2015 results. XIX. Constraints on primordial magnetic fields, Astron. Astrophys. **594**, A19 (2016).
- [21] C. T. Byrnes, P. S. Cole, and S. P. Patil, Steepest growth of the power spectrum and primordial black holes, J. Cosmol. Astropart. Phys. 06 (2019) 028.
- [22] P. Carrilho, K. A. Malik, and D. J. Mulryne, Dissecting the growth of the power spectrum for primordial black holes, Phys. Rev. D 100, 103529 (2019).
- [23] O. Özsoy and G. Tasinato, On the slope of the curvature power spectrum in non-attractor inflation, J. Cosmol. Astropart. Phys. 04 (2020) 048.
- [24] G. Tasinato, An analytic approach to non-slow-roll inflation, Phys. Rev. D 103, 023535 (2021).
- [25] M. Cielo, G. Mangano, O. Pisanti, and D. Wands, Steepest growth in the primordial power spectrum from excited states at a sudden transition, J. Cosmol. Astropart. Phys. 04 (2025) 007.
- [26] G. Tasinato, Large $|\eta|$ approach to single field inflation, Phys. Rev. D **108**, 043526 (2023).
- [27] S. Matarrese, O. Pantano, and D. Saez, A general relativistic approach to the nonlinear evolution of collisionless matter, Phys. Rev. D 47, 1311 (1993).
- [28] K. N. Ananda, C. Clarkson, and D. Wands, The cosmological gravitational wave background from primordial density perturbations, Phys. Rev. D 75, 123518 (2007).
- [29] D. Baumann, P. J. Steinhardt, K. Takahashi, and K. Ichiki, Gravitational wave spectrum induced by primordial scalar perturbations, Phys. Rev. D 76, 084019 (2007).
- [30] R. Saito and J. Yokoyama, Gravitational-wave constraints on the abundance of primordial black holes, Prog. Theor. Phys. **123**, 867 (2010).
- [31] E. Bugaev and P. Klimai, Induced gravitational wave background and primordial black holes, Phys. Rev. D 81, 023517 (2010).
- [32] J. R. Espinosa, D. Racco, and A. Riotto, A cosmological signature of the SM Higgs instability: Gravitational waves, J. Cosmol. Astropart. Phys. 09 (2018) 012.
- [33] K. Kohri and T. Terada, Semianalytic calculation of gravitational wave spectrum nonlinearly induced from primordial curvature perturbations, Phys. Rev. D **97**, 123532 (2018).
- [34] G. Domènech, Scalar induced gravitational waves review, Universe 7, 398 (2021).
- [35] G. Domènech, S. Passaglia, and S. Renaux-Petel, Gravitational waves from dark matter isocurvature, J. Cosmol. Astropart. Phys. 03 (2022) 023.

- [36] S. Passaglia and M. Sasaki, Primordial black holes from CDM isocurvature perturbations, Phys. Rev. D 105, 103530 (2022).
- [37] G. Domènech, Cosmological gravitational waves from isocurvature fluctuations, AAPPS Bull. **34**, 4 (2024).
- [38] O. Ozsoy and G. Tasinato, Vector dark matter, inflation, and non-minimal couplings with gravity, J. Cosmol. Astropart. Phys. 06 (2024) 003.
- [39] A. Marriott-Best, M. Peloso, and G. Tasinato, New gravitational wave probe of vector dark matter, Phys. Rev. D 111, 103511 (2025).
- [40] R. Durrer, P.G. Ferreira, and T. Kahniashvili, Tensor microwave anisotropies from a stochastic magnetic field, Phys. Rev. D 61, 043001 (2000).
- [41] C. Caprini and R. Durrer, Gravitational wave production: A strong constraint on primordial magnetic fields, Phys. Rev. D 65, 023517 (2001).
- [42] A. Mack, T. Kahniashvili, and A. Kosowsky, Microwave background signatures of a primordial stochastic magnetic field, Phys. Rev. D 65, 123004 (2002).
- [43] L. Pogosian, T. Vachaspati, and S. Winitzki, Signatures of kinetic and magnetic helicity in the CMBR, Phys. Rev. D 65, 083502 (2002).
- [44] C. Caprini, R. Durrer, and T. Kahniashvili, The cosmic microwave background and helical magnetic fields: The tensor mode, Phys. Rev. D 69, 063006 (2004).
- [45] J. R. Shaw and A. Lewis, Massive neutrinos and magnetic fields in the early universe, Phys. Rev. D 81, 043517 (2010).
- [46] S. Saga, H. Tashiro, and S. Yokoyama, Limits on primordial magnetic fields from direct detection experiments of gravitational wave background, Phys. Rev. D 98, 083518 (2018).
- [47] A. Bhaumik, T. Papanikolaou, and A. Ghoshal, Vector induced gravitational waves sourced by primordial magnetic fields, J. Cosmol. Astropart. Phys. 08 (2025) 054.
- [48] S. Maiti, D. Maity, and R. Srikanth, Probing reheating phase via non-helical magnetogenesis and secondary gravitational waves, arXiv:2505.13623.
- [49] K. Subramanian, Magnetic fields in the early universe, Astron. Nachr. 331, 110 (2010).
- [50] A. Karam, N. Koivunen, E. Tomberg, V. Vaskonen, and H. Veermäe, Anatomy of single-field inflationary models for primordial black holes, J. Cosmol. Astropart. Phys. 03 (2023) 013.
- [51] G. Franciolini and A. Urbano, Primordial black hole dark matter from inflation: The reverse engineering approach, Phys. Rev. D 106, 123519 (2022).
- [52] G. 't Hooft, A planar diagram theory for strong interactions, Nucl. Phys. B72, 461 (1974).
- [53] G. Tasinato, Non-Gaussianities and the large |η| approach to inflation, Phys. Rev. D 109, 063510 (2024).
- [54] K. Jedamzik, V. Katalinic, and A. V. Olinto, Damping of cosmic magnetic fields, Phys. Rev. D 57, 3264 (1998).
- [55] M. Mylova, O. Özsoy, S. Parameswaran, G. Tasinato, and I. Zavala, A new mechanism to enhance primordial tensor fluctuations in single field inflation, J. Cosmol. Astropart. Phys. 12 (2018) 024.
- [56] O. Ozsoy, M. Mylova, S. Parameswaran, C. Powell, G. Tasinato, and I. Zavala, Squeezed tensor non-Gaussianity in non-attractor inflation, J. Cosmol. Astropart. Phys. 09 (2019) 036.

- [57] H. A. G. Cruz, T. Adi, J. Flitter, M. Kamionkowski, and E. D. Kovetz, 21-cm fluctuations from primordial magnetic fields, Phys. Rev. D 109, 023518 (2024).
- [58] D. Paoletti, J. Chluba, F. Finelli, and J. A. Rubiño-Martin, Constraints on primordial magnetic fields from their impact on the ionization history with Planck 2018, Mon. Not. R. Astron. Soc. 517, 3916 (2022).
- [59] J. Chluba, D. Paoletti, F. Finelli, and J.-A. Rubiño-Martín, Effect of primordial magnetic fields on the ionization history, Mon. Not. R. Astron. Soc. 451, 2244 (2015).
- [60] G. Tasinato, A scenario for inflationary magnetogenesis without strong coupling problem, J. Cosmol. Astropart. Phys. 03 (2015) 040.
- [61] C. Caprini, R. Jinno, M. Lewicki, E. Madge, M. Merchand, G. Nardini, M. Pieroni, A. Roper Pol, and V. Vaskonen (LISA Cosmology Working Group Collaboration), Gravitational waves from first-order phase transitions in LISA: Reconstruction pipeline and physics interpretation, J. Cosmol. Astropart. Phys. 10 (2024) 020.
- [62] J. J. Blanco-Pillado, Y. Cui, S. Kuroyanagi, M. Lewicki, G. Nardini, M. Pieroni, I. Y. Rybak, L. Sousa, and J. M. Wachter (LISA Cosmology Working Group Collaboration), Gravitational waves from cosmic strings in LISA: Reconstruction pipeline and physics interpretation, J. Cosmol. Astropart. Phys. 05 (2025) 006.
- [63] M. Braglia et al. (LISA Cosmology Working Group Collaboration), Gravitational waves from inflation in LISA: Reconstruction pipeline and physics interpretation, J. Cosmol. Astropart. Phys. 11 (2024) 032.
- [64] M. Colpi *et al.* (LISA Collaboration), LISA definition study report, arXiv:2402.07571.
- [65] K. Schmitz, New sensitivity curves for gravitational-wave signals from cosmological phase transitions, J. High Energy Phys. 01 (2021) 097.
- [66] D. Chowdhury, G. Tasinato, and I. Zavala, The rise of the primordial tensor spectrum from an early scalar-tensor epoch, J. Cosmol. Astropart. Phys. 08 (2022) 010.
- [67] A. Marriott-Best, D. Chowdhury, A. Ghoshal, and G. Tasinato, Exploring cosmological gravitational wave backgrounds through the synergy of LISA and the Einstein Telescope, Phys. Rev. D 111, 103001 (2025).
- [68] R.-G. Cai, S. Pi, and M. Sasaki, Universal infrared scaling of gravitational wave background spectra, Phys. Rev. D 102, 083528 (2020).
- [69] C. Caprini, D. G. Figueroa, R. Flauger, G. Nardini, M. Peloso, M. Pieroni, A. Ricciardone, and G. Tasinato, Reconstructing the spectral shape of a stochastic gravitational wave background with LISA, J. Cosmol. Astropart. Phys. 11 (2019) 017.
- [70] P. Auclair *et al.* (LISA Cosmology Working Group Collaboration), Cosmology with the Laser Interferometer Space Antenna, Living Rev. Relativity **26**, 5 (2023).
- [71] J. E. Gammal *et al.* (LISA Cosmology Working Group Collaboration), Reconstructing primordial curvature perturbations via scalar-induced gravitational waves with LISA, J. Cosmol. Astropart. Phys. 05 (2025) 062.
- [72] A. Ghaleb, A. Malhotra, G. Tasinato, and I. Zavala, Bayesian reconstruction of primordial perturbations from induced gravitational waves, arXiv:2505.22534.